

## Development of a Design Tool for Gas Separation Membrane Modules using Computational Fluid Dynamics Simulation

Hiromitsu Takaba, Takuro Nishimura\*, Kimito Funatsu\* and Shin-ichi Nakao

Department of Chemical System Engineering, The University of Tokyo, 7-3-1 Hongo, Bunkyo-ku, 113-8656 Tokyo  
Fax: +81-3-5841-7300, e-mail: takaba@chemsys.t.u-tokyo.ac.jp

\* Department of Knowledge-based Information Engineering, Toyohashi University of Technology,  
Hibarigaoka 1-1, Tempaku, 441 Toyohashi  
Fax: +81-532-47-9315, e-mail: funatsu@tutkie.tut.ac.jp

A design tool for gas membrane modules using computational fluid dynamics (CFD) was developed. This tool consists of two modules and a user-interface; the structure generator module, the optimization module for automatic optimization of the structural parameters of the module based on a genetic algorithm, and the CFD simulator. The CFD simulator was applied to modeling the  $H_2$  selective extraction from an  $H_2/CO$  gas mixture using a tube-type ceramic membrane in the steam reforming process. The calculated results were compared with the experimental result to test the validity of CFD simulator for simulating the concentration polarization. Calculated modulus of the concentration polarization was in good agreement with the experimental results, suggesting that the validity of CFD simulator to predict the performance of gas separation membrane modules.

Key words: gas separation, computational fluid dynamics, concentration polarization, membrane module

### 1. INTRODUCTION

A general model of a membrane module, applicable to pressure driven membrane processes, has been developed based on the permeation model; however, most assume ideal gas flow, which will sometimes overestimate, or underestimate, performance. This error is caused partially by non-ideal flow that is a function of scale or the geometry of the module. In addition to non-ideal fluid dynamics, the concentration polarization of preferable permeation gas is an important factor that determines the performance of the module, which is difficult to consider in general models.

Haraya et al. [1] reported experiments showing that the polarization effect in pressure-driven gas permeation in the membrane is significant when the permeability of the membrane used is greater than  $2.4 \times 10^{-6} \text{ mol m}^{-2} \text{ s}^{-1} \text{ Pa}^{-1}$  and the separation factor is approximately two. He et al. [2] reported a theoretical study in which they describe how the concentration polarization becomes significant when the flux is greater than  $3 \times 10^{-7} \text{ mol m}^{-2} \text{ s}^{-1} \text{ Pa}^{-1}$ .

Recently, Wiley et al. [3] reported a computational fluid dynamics (CFD) study on pressure-driven membrane processes involving selective component rejection with concentration polarization on the membrane surface. Their CFD study modeled an ultrafiltration membrane for selective removal of components in the feed. Koukou et al. [4] performed a CFD simulation for a concentration polarization on a pressure-driven gas separation processes using a two-dimensional model, which was in agreement with their experimental data. However, a full computational study of the conditions of the concentration polarization in gas separation membranes has not been performed.

This paper presents our attempt to rationalize the design of membrane modules optimized for particular operating conditions based on CFD simulation combined with optimization. This tool provides a user interface that combines the CFD simulator with the optimization tool and the structure generator. In this article, we introduce this tool briefly and present the result of testing the validity of the CFD simulator for modeling gas permeation through a membrane.

### 2. MEMBRANE DESIGN TOOL

Fig. 1 shows our membrane design tool, which consists of three individual tools:

- the CFD simulator, which calculates the fluid dynamics in a given module geometry based on the input data;

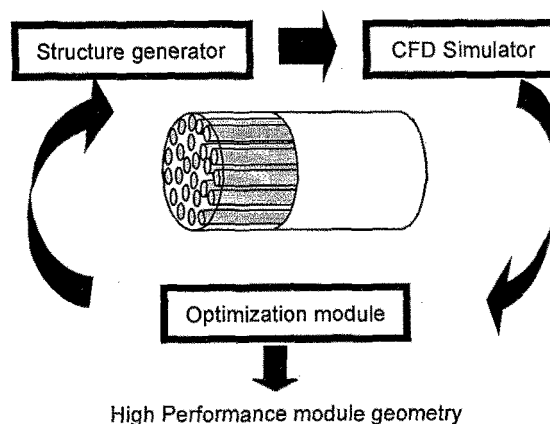


Fig. 1 Schematic representation of a design tool for membrane module

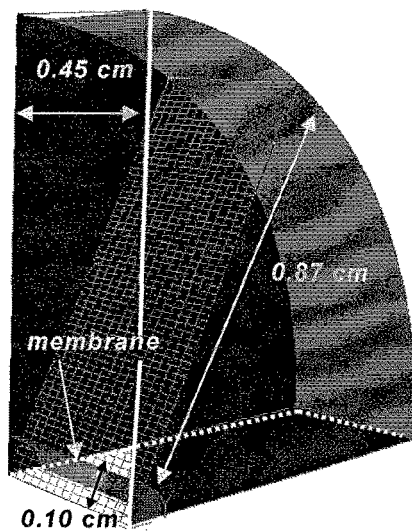


Fig. 2 Schematic representation of geometry models.

- the user-interface of structure generator for generating a structure as an input file for the CFD simulator, which enables the input of an operating condition, and selection and coordination of elements, such as a location of inlet/outlet, flow type (co-counter current or counter-current models) and the size of both module and membranes;
- the optimization module that generates alternative input data, based on the CFD result, which would give better performance.

The surface area, coordination of inlet/outlet, and the size of the module are optimization parameters. The performance of the module is evaluated by two output-parameters from the CFD simulator: the recovery ratio and the separation factor. This sequence of the optimization tool and CFD simulator is repeated until the calculated performance of the module satisfies a target performance.

### 3. CFD SIMULATION DETAIL

The CFD calculation is performed based on the differential equations for all variables, which are as follows [4]:

$$\frac{\partial(\rho\Phi)}{\partial t} + \text{div}(\rho\vec{u}\Phi - \Gamma_{\Phi}\text{grad}\Phi) = S_{\Phi} \quad (1)$$

where  $\rho$  is the density of the mixture gas,  $\Phi$  is the dependent variable,  $\vec{u}$  is the velocity vector,  $\Gamma_{\Phi}$  is the appropriate coefficient for variable  $\Phi$ , which in the mass fraction equation is calculated as  $\Gamma_{\Phi} = \rho D$ .  $D$  is the diffusion coefficient, and  $S_{\Phi}$  is the source-sink term per unit volume for variable  $\Phi$ .  $\rho$  is calculated using the ideal gas law as:

$$\rho = \frac{PM}{RT} \quad (2)$$

where  $P$  is the total pressure,  $R$  is the gas constant,  $T$  is

Table 1 The Flow properties and operating variables.

geometry model	Tube
permeability of $H_2$ [ $\times 10^{-6} \text{ mol m}^{-2} \text{ s}^{-1} \text{ Pa}^{-1}$ ]	10 <sup>-3</sup> -10
selectivity ( $H_2/CO$ )	3.74
pressure in the feed side [MPa]	1.1
pressure in the permeate side [MPa]	0.1-0.6
kinematic viscosity of gas [ $10^{-6} \text{ m}^2 \text{ s}^{-1}$ ]	2.54 at 1.1 MPa
molar ratio of the feed mixture gas ( $H_2:CO$ )	1:1
Feed velocity [ $10^{-2} \text{ m s}^{-1}$ ]	2.05-4.10
Temperature [K]	373

the temperature, and  $M$  is the molar weight of the gas mixture. The above set of equations is solved numerically based on the finite volume method embedded in the PHOENICS package [5]. The entire region is discretized into a grid of finite control volume cells.

Tube geometry was considered for the model of the membrane module in the CFD calculations, as shown in Figure 2. The model represents a quarter of the volume of the permeable section of the entire membrane module as reported by Haraya et al. [1]. The feed mixture gas is introduced to the permeation cell, and selectively permeates from the permeation cell to the capillary tube located at the center of the module. The retentate and permeated gases come from the outlet, which is placed on the opposite side to the inlet. In the experiment [1], the capillary porous glass membrane having the small permeable area was carefully placed at a point apart from the gas inlet and outlet, to eliminate the influence of velocity disturbance. Although the CFD calculation considers only part of the permeation cell, the condition of flow would be similar because the gas velocity is uniform and perpendicular to the inlet surface and is given at the inlet in the calculations.

The operating condition models for separation of  $H_2$  from stream reforming gas ( $H_2/CO$  mixture gas) were: the flow was assumed to be steady state, laminar and incompressible. The flow properties and operating variables are summarized in Table 1.

### 4. RESULTS AND DISCUSSION

To test the validity of the CFD for quantitative estimation of concentration polarization, the CFD calculation was performed using the same conditions as the experiment described by Haraya et al. [1]. In the experiment, the flux and selectivity were measured with the change of the feed pressure, the size of the permeation cell, and the membrane length. Calculation

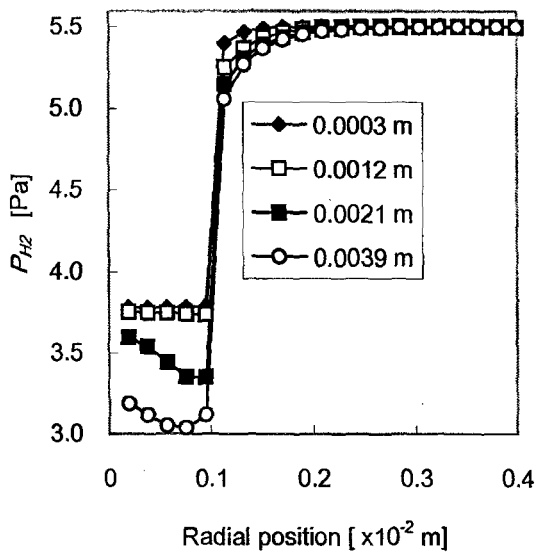


Fig. 3 The profiles of  $P_{H_2}$  at different slice positions. The zero slice position is at the inlet. The permeate side occupied between 0.00 - 0.10 in the radial position and the feed side occupied 0.10 - in the radial position.

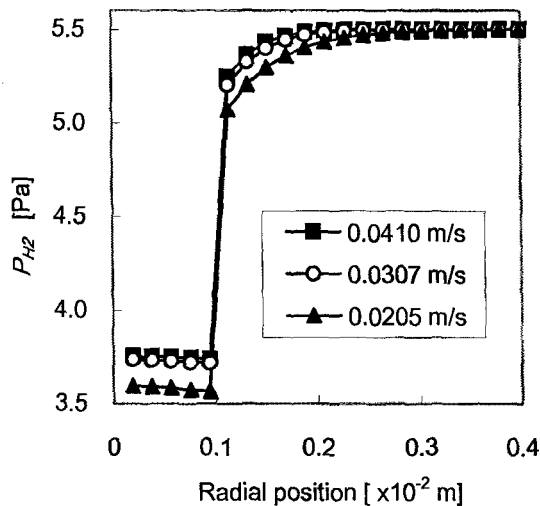


Fig. 4 Changes of the profiles of  $P_{H_2}$  at the slice positions of  $0.12 \times 10^{-2}$  m for various feed velocities. The permeate side occupied between 0.00 - 0.10 in the radial position and the feed side occupied 0.10 - in the radial position.

was performed in one of those conditions; the diameter of the permeation cell was  $1.92 \times 10^{-2}$  m, the tube diameter was  $0.19 \times 10^{-2}$  m, the flux was  $0.41 \times 10^{-2}$  m s<sup>-1</sup>, and the membrane length  $0.45 \times 10^{-2}$  m.

Fig. 3 shows the profile of the  $p_{H_2}$  in a slice through the module when the feed velocity was  $4.10 \times 10^{-2}$  m. The slice position is along the axial direction of the

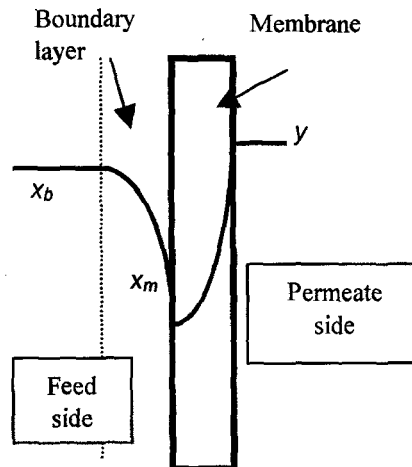


Fig. 5 Schematic figure of concentration polarization.

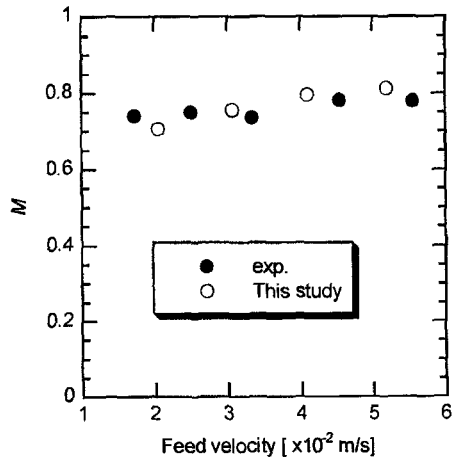


Fig. 6 Comparison of the modulus of concentration polarization obtained by CFD and experimentally [1].

module. The inner tube-type membrane was located at  $0.10 \times 10^{-2}$  m in the radial position. The  $p_{H_2}$  in the feed side gradually decreases close to the membrane, although they are constant away from the membrane; concentration polarization is observed in these profiles. In comparison to the slice position, the decline of  $p_{H_2}$  becomes large close to the outlet, and this is because of the decrease of the driving pressure for the permeation of  $H_2$ . Total flux of  $H_2$  becomes large close to the outlet and the decrease of  $H_2$  pressure at the membrane surface was not compensated with the mass transport by gas diffusion of  $CO_2$  perpendicular to the membrane. In the permeate side,  $p_{H_2}$  decreases as the slice position nears the outlet, and at slice positions greater than  $0.2 \times 10^{-2}$  m a dramatic decline of  $p_{H_2}$  at the membrane is observed, this results from the high flux of  $CO$  at those positions.

The concentration polarization is a function of feed velocity, and the CFD result for changing feed velocity is shown in Fig. 4. The slice positions of the indicated

profiles are  $0.12 \times 10^{-2}$  m. The decline of  $p_{H_2}$  at the membrane is observed in all profiles, which means that a concentration polarization occurs, although the profiles of  $p_{H_2}$  for the feed velocity of  $4.10 \times 10^{-2}$  and  $3.07 \times 10^{-2}$  m are similar. For the profile of  $2.05 \times 10^{-2}$  m,  $p_{H_2}$  the decline close to the membrane is remarkable, and in the permeate side it's magnitude is significantly small. This is due to a concentration polarization that decreases the flux of the more permeable gas.

Fig. 5 is the schematic representation of the concentration polarization.  $x_b$  and  $x_m$  are the mole fraction of  $H_2$  in the feed side and at the membrane, respectively.  $y$  is the mole fraction of  $H_2$  on the permeate side. Considering this representation, a modulus of concentration polarization,  $M$ , can be defined as [1]:

$$M = \frac{y - x_b}{y - x_m} \quad (3)$$

$M$  is always less than one when concentration polarization takes place. The  $M$  calculated from the CFD result is shown in Fig. 6 with the experimental result [1]. In the experiment,  $M$  slightly increased with increasing  $F$  and the trend for  $M$  corresponds with that obtained by CFD. Although the slight discrepancy between  $M$  obtained by CFD and experimentally is observed when the feed velocity is small, the CFD result is in good agreement with the experimental result. This suggests the validity of the CFD simulation for evaluation of concentration polarization in a membrane module for gas separation. It has been reported that the estimation of  $M$  in the experiment included some error because of the uncertain assumption of the estimation of mean radius of the concentration boundary layer [1].

## 5. CONCLUSION

The CFD calculation of  $H_2/CO$  permeation through the membranes was performed using the tube geometry model with the same conditions as the experiment of Haraya et al. [1]. The concentration polarization observed in CFD simulation compared well with that reported experimentally. This suggests the CFD simulator can be used to design a membrane module involving prediction of selectivity and cut.

## 6. ACKNOWLEDGEMENT

This work was by NEDO as a part of the R&D Project for High Efficiency Hydrogen Production/Separation System using Ceramic Membrane promoted by METI, Japan.

## 7. REFERENCES

- [1] K. Haraya, T. Hakuta and H. Yoshitome, *Sep. Sci. Tech.*, 22, 1425-1438 (1987).
- [2] G. He, Y. Mi, P. L. Yue and G. Chen, *J. Membrane Sci.*, 153, 243-258 (1999).
- [3] D. Willey and D. F. Fletcher, *Desalination*, 145, 183-186 (2002).
- [4] M. K. Koukou, N. Papayannakos, N. C. Markatos, M. Bracht, H. M. Van Veen and A. Roskam, *J. Membr. Sci.*, 155, 241-259 (1999).

155, 241-259 (1999).

[5] S. V. Patankar, *Numerical Heat Transfer and Fluid Flow*, Hemisphere Publishing Corporation, New York, (1980).

[6] C. T. Blaisdell and K. Kammermeyer, *Chem. Eng. Sci.*, 28, 1249-1255 (1973).

(Received October 13 2003; Accepted March 31, 2004)